

COSMIC RAY ANTIPROTONS

DALLAS C. KENNEDY

Department of Physics, University of Florida, Gainesville FL 32611, USA
E-mail: kennedy@phys.ufl.edu •• WWW: http://www.phys.ufl.edu/~kennedy

Cosmic ray antiprotons have been detected for over 20 years and are now measured reliably. Standard particle and astrophysics predict a conventional spectrum and abundance of secondary antiprotons consistent with all current measurements. These measurements place limits on exotic Galactic antiproton sources and non-standard antiproton properties. Complications arise, particularly at low energies, with heliospheric modulation of cosmic ray fluxes and production of standard secondaries from $A > 1$ nuclear targets. Future experiments and theoretical developments are discussed.

1 General Properties of Cosmic Rays

Cosmic rays are high-energy p , \bar{p} , nuclei, and e^\pm in interplanetary and interstellar (IS) space. The dominant component consists of protons (hydrogen H) with a smaller admixture of heavier nuclei, especially He (Figure 1). Antiprotons (\bar{p}) occur at an abundance of $10^{-4,-5}$ times that of p . These energetic particles, with kinetic energy $K > 10$ MeV, are Galactic in origin, not to be confused with the much denser solar wind plasma, with much lower K , streaming from the Sun.^a

The relative element abundances in cosmic rays (CRs) indicate they originate in the IS medium, where they are ionized and accelerated, probably by supernova shocks. (Recent measurements all but rule out an origin in supernova ejecta proper.) Such accelerated, pre-existing nuclei are CR *primaries*.¹ Once accelerated to high energies, the primaries induce the production of further CRs, the *secondaries*, in the IS medium and at local sites in the Galaxy. (The terms “primaries” and “secondaries” are also used in a completely different sense: CR primaries are the CRs that strike the top of the Earth’s atmosphere, the secondaries the induced CR shower propagating into the lower atmosphere.) Secondaries include e^+ , \bar{p} , and certain nuclear isotopes. As some of these isotopes are unstable, their populations must be continually replenished to maintain their observed abundances.

^aAlso ignored here are “pickup ions” or anomalous Galactic cosmic rays, neutral IS atoms which drift into the solar system and are then ionized by solar UV radiation.

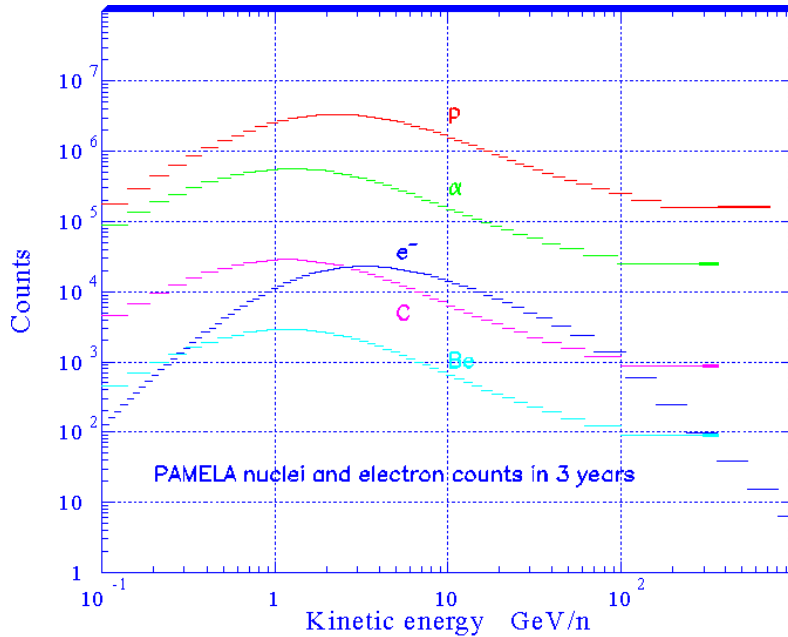


Figure 1. Typical cosmic ray matter spectrum: isotopic count spectra expected for orbital PAMELA instrument (see text) over 3 years = 95 Msec. Isotopes shown: H, He, Be, and C, as well as electrons e^- .²

1.1 Cosmic Ray Antiprotons

Standard secondary CR antiprotons are produced by the process $pA \rightarrow \bar{p}X$, with p = high-energy CR, A = IS medium nucleus of atomic weight A , and X = anything consistent with charge and baryon number (B) conservation. The threshold channel is $pA \rightarrow p\bar{p}pA$, with threshold $E_p = (3 + 4/A)m_p$. (The nucleus A can break up without significantly changing the dynamics.) The dominant case is H, $A = 1$, with threshold $E_p = 7m_p$. The only other significant contribution comes from He target nuclei. By number, the IS medium is $\simeq 93\%$ H and 7% He.^{3,4,5,6,7}

The secondary \bar{p} 's subsequently propagate in the Galaxy and are subject to a variety of elastic (scattering, including energy-loss) and inelastic (annihilation and extra-Galactic leakage) processes. Leakage is the dominant loss; the Galactic storage time ~ 13 Myr as inferred from the abundance of unstable CR isotopes. Energy loss shifts the \bar{p} spectrum without changing their number.

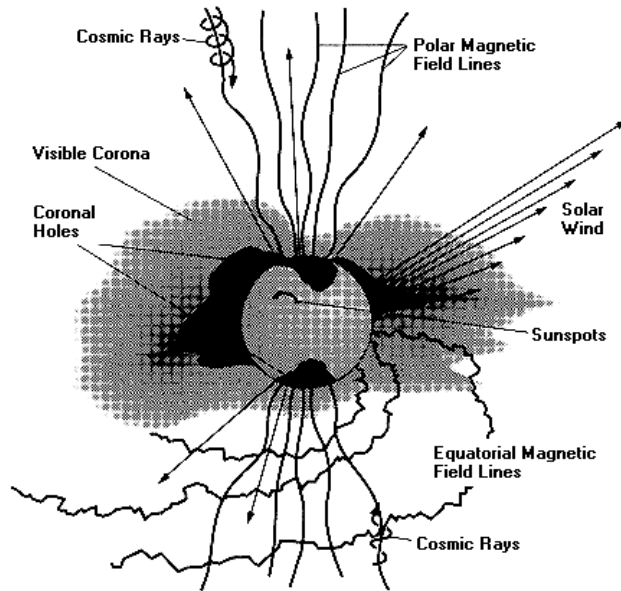


Figure 2. Galactic cosmic rays propagate into heliosphere by spiraling along heliomagnetic field lines, but the field itself also fluctuates randomly. Solar wind also convects and decelerates incoming cosmic rays. ¹⁵

Some uncertainty is unavoidable in models of Galactic propagation, including H and He abundances, as well as the Galaxy's highly tangled, stochastic magnetic field $B_{\text{Gal}} \sim 0.3 \text{ nT}$ and small wind $V_{\text{Gal}} \lesssim 20 \text{ km sec}^{-1}$ (a superposition of many stellar and supernova winds). The field and wind control the diffusion of CRs into intergalactic space and are fairly well constrained by measurements of unstable CR isotopes. But more complicated transport mechanisms are possible, including reacceleration shocks and variation of the Galactic geometry. ^{7,8,9,10}

The CR fluxes measured at the top of the Earth's atmosphere are modulated by their transport through the heliosphere, the Sun's magnetic sphere of influence (Figure 2). The heliosphere consists of a solar wind ($V_W \simeq 400 \text{ km sec}^{-1}$ along the ecliptic plane, $700\text{-}800 \text{ km sec}^{-1}$ along the solar axes) of e^- and nuclei (mainly p) carrying the embedded magnetic field B_{\odot} (Figure 2). Near the Sun, the field falls off with heliocentric distance r as r^{-2} , arising from frozen field flux transported radially outwards. Since the Sun rotates, however, the field is twisted into an Archimedean or *Parker spiral*,

and the field is predominantly azimuthal in the outer solar system, falling off more softly as r^{-1} . At one AU (AU = 149.5 Mkm, the Earth's orbit), the heliomagnetic field strength $B_{\odot} \simeq 5$ nT. ¹¹

The CRs gyrate around the local \mathbf{B} field lines. The solar field is not fully deterministic, however: it is modified by episodic (practically random) shocks that cause the CRs to diffuse along and across field lines, especially at times of solar magnetic maximum (currently 2000-01 and periodically about every 11 years, when the heliomagnetic field changes sign). In addition, the wind both imposes a macroscopic convective drift and performs work on the CRs (adiabatic deceleration), lowering their energies as they fight “upstream” into the inner solar system. A realistic prediction of Earth-measured CR fluxes must include these mechanisms, which are particularly important at lower K and affect oppositely-charged CRs differently. ^{12,13,9} Heliospheric *in situ* measurements have been ongoing for four decades and have recently become much better with the *IMP* and *Ulysses* space probes. ^{14,15}

1.2 Exotic Sources of Cosmic Ray Antiprotons

The density of IS matter $n_{\text{H}} \sim 1$ H atom cm^{-3} and the known spectrum and abundance of CR p primaries fix the predicted spectrum and abundance of \bar{p} secondaries, if the $pA \rightarrow \bar{p}X$ cross section $\sigma(\bar{p})$ is known. ⁴ Let $Q_{\bar{p}}(K)$ be the differential production rate (antiprotons $\text{cm}^{-3} \text{MeV}^{-1} \text{sec}^{-1}$); schematically,

$$Q_{\bar{p}}(K) = \int dK' n_p(K') v(p) n_{\text{H}} \cdot d\sigma(pp \rightarrow \bar{p}; K, K') / dK' \quad . \quad (1)$$

The pp process has been measured in laboratory experiments, and the $p+\text{He}$ case can be inferred from the pp cross section (but see subsection 3.2). The differential \bar{p} abundance $n_{\bar{p}}(K)$ (antiprotons $\text{cm}^{-3} \text{MeV}^{-1}$) is related to $Q_{\bar{p}}(K)$ by $n_{\bar{p}}(K) = \tau_{\text{eff}}(K) \cdot Q_{\bar{p}}(K)$, where the effective Galactic residence time

$$\frac{1}{\tau_{\text{eff}}(K)} = \frac{1}{\tau_{\text{leak}}(K)} + \frac{1}{\tau_{\text{ann}}(K)} + \dots \quad , \quad (2)$$

summing over all loss mechanisms. The sum is dominated by the first term, the extra-Galactic diffusion rate. The measured CR \bar{p} flux is then related to $n_{\bar{p}}(K)$ through the transformation by heliospheric transport. Variation of Galactic transport mechanisms modifies $\tau_{\text{eff}}(K)$. This picture is the basis for the simple *Leaky Box Model*. A more complex picture, with explicit spatial dependence on Galactic geometry (inhomogeneous leaky disk model = ILDM), is possible and indeed necessary, because of measurements of Galactic plane cosmic ray synchrotron radiation mapping the IS CR distribution. ^{16,8,10}

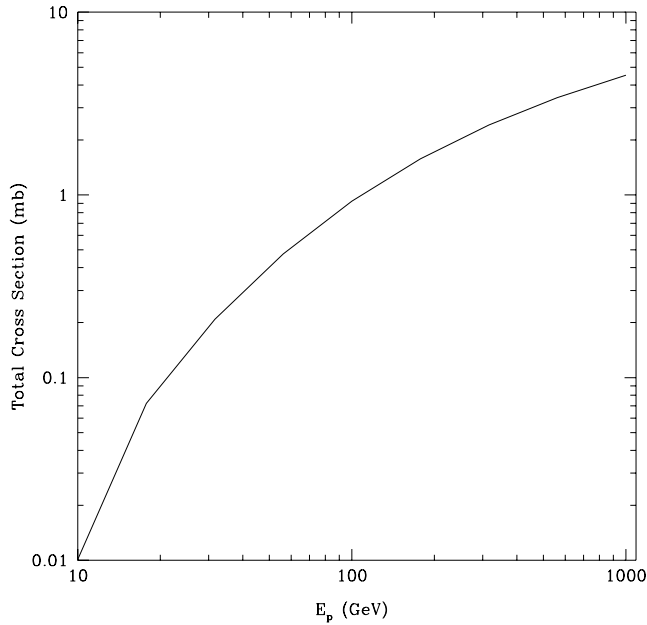


Figure 3. The total $pp \rightarrow \bar{p}X$ cross section as a function of incident p total energy in target p rest frame. Based on measured cross section and semianalytic representation by Stephens.⁴

The cross section $\sigma(\bar{p})$ has a crucial property arising from its threshold at $E_p = 7m_p$ (Figure 3). The spectrum of outgoing \bar{p} 's rises sharply from $K_{\bar{p}} = 0$. Since $n_p(K)$ falls off rapidly (as $K_{\bar{p}}^{-2.75}$), $n_{\bar{p}}(K)$ falls off similarly at high $K_{\bar{p}}$, leaving a \bar{p} secondary spectrum with a sharp rise to a peak at $K \sim 2$ GeV and falling off above that. The lower threshold for He targets enhances the low- K spectrum somewhat.

Although the secondary \bar{p} spectrum must be there, its presence does not rule out non-standard \bar{p} sources, so-called “exotic primaries”. These would add to the predicted secondary flux in total number. More crucially, they can also change the *shape* of the \bar{p} spectrum, particularly at low K , as well the fall-off for $K \gtrsim 3$ GeV. Cosmologically significant amounts of antimatter are strongly disfavored.¹⁷ Instead, the most logical sources for trace amounts of exotic primary \bar{p} would be annihilating or decaying dark matter remnants in the halo of our Galaxy. Popular models feature annihilating supersymmetric (SUSY) dark matter^{18,19,20,21} (WIMPs, assumed to be the LSP = lightest

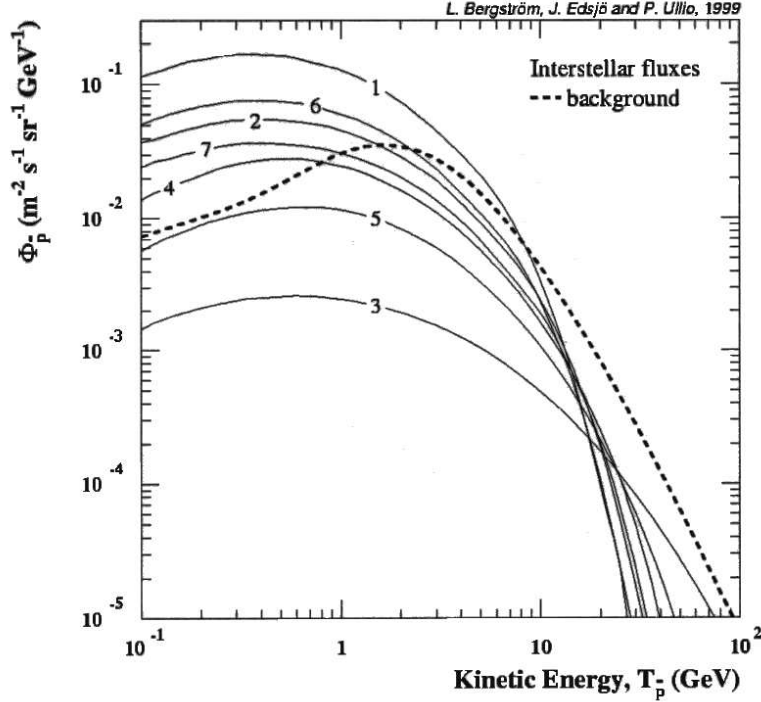


Figure 4. A range of minimal (R-parity-conserving) SUSY predictions of Galactic \bar{p} spectrum, with neutralino mass $m_{\tilde{\chi}^0} = 45\text{--}700$ GeV and standard secondaries = “background”. Adapted from work of Bergström, Edsjö, and Ullio.²³

SUSY particle, usually neutralinos $\tilde{\chi}^0$) or decaying primordial black holes.^{22,4} The predictions depend on model details,^{10,23,24} but both have roughly flat \bar{p} production spectra as $K \rightarrow 0$ and a non-standard fall-off with K at high energies. Such signals can only be seen if the exotic primaries compete in number with standard secondaries. A general range of exotic SUSY \bar{p} production (Figure 4) exhibits the dramatic modification of the low- K \bar{p} spectrum possible in SUSY CDM models of the Galactic halo for smaller neutralino mass.

SUSY halo dark matter \bar{p} 's (from $\tilde{\chi}^0\tilde{\chi}^0 \rightarrow q\bar{q}$, Figure 5a) requires sufficient abundance and a large enough annihilation cross section to be seen, in turn implying WIMP masses \lesssim few 100 GeV and $\sigma(\text{ann})v(\text{WIMP}) \sim 0.1$ pb.

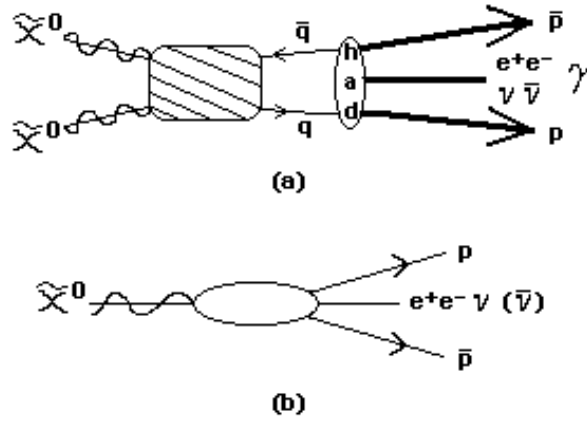


Figure 5. Supersymmetric CDM LSPs as a source of CR \bar{p} 's. (a) CDM neutralinos $\tilde{\chi}^0$'s annihilate in the Galactic halo in minimal SUSY. (b) In R-parity-violating SUSY, neutralinos $\tilde{\chi}^0$'s can also decay by $\Delta L \neq 0$ channels.

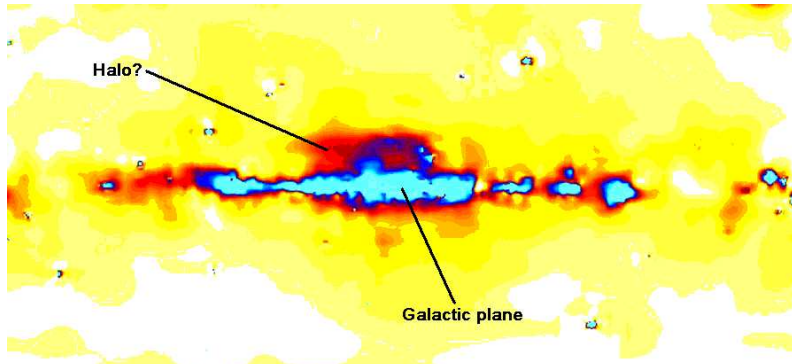


Figure 6. Intensity map of Galactic γ rays: most intense is central, horizontal Galactic plane, with possible fainter Galactic halo emission. EGRET/Compton Gamma Ray Observatory. ²⁶

(Production of heavier WIMPs is suppressed in the Big Bang with increasing mass.) The hadronic shower evolves finally into p 's, \bar{p} 's, e^\pm , ν 's, and

γ 's. WIMP annihilation is natural in minimal SUSY models with conserved R -parity. An extension of minimal SUSY allows R -parity violation, in turn allowing the LSPs to decay to ordinary matter, violating lepton and/or baryon number (Figure 5b). This mechanism could open another source of CR \bar{p} 's. In a semi-realistic scenario, ²⁵ lepton number violation is dominant, leading in the end to excess (anti)neutrinos. An exciting possible signal of annihilating or decaying CDM in the Galactic halo is suggested by the Galactic gamma ray maps of the orbiting Compton Gamma Ray Observatory's EGRET telescope (Figure 6).

Primordial black holes (PBHs) are postulated to have been produced very early in the hot Big Bang, in the quantum gravity era. ²² They evaporate in turn by the Hawking process, as their temperatures rise, and can produce significant p 's and \bar{p} 's at a late time when $T_{\text{BH}} \gtrsim \Lambda_{\text{QCD}}$. The relic PBH density and \bar{p} production rate have been estimated. ²⁴

1.3 Intrinsic Properties of Antimatter: CPT Symmetry

Cosmic ray \bar{p} 's also give us a window on the intrinsic properties of antimatter. These properties should be the same or charge-conjugated from the corresponding matter by the CPT (charge-conjugation, parity- and time-reversal) symmetry of local relativistic quantum field theory (LRQFT). Some \bar{p} properties have been checked in the laboratory directly. These include the mass, charge, magnetic moment, and the neutrality of hydrogen and antihydrogen. ²⁷

More difficult to limit is the decay lifetime of \bar{p} 's. Not enough antimatter can be gathered into a detector for long enough to produce lifetime limits on antimatter competitive with the limits for matter. Astrophysical processes partially ameliorate this difficulty. The Galactic storage time for \bar{p} 's ~ 10 Myr, and intrinsic \bar{p} decay would modify the Galactic residence time τ_{eff} . If the decay lifetime is short enough (taking Lorentz dilation into account), the \bar{p} spectrum is significantly distorted. The shape and normalization of the \bar{p} spectrum then place a lower limit on $\tau_{\bar{p}}$. ²⁸

Laboratory limits have been obtained for the \bar{p} lifetime. Earlier limits include the LEAR Collaboration at the CERN \bar{p} storage ring ($\tau_{\bar{p}} > 0.08$ yr) and the antihydrogen Penning trap of Gabrielse *et al.* ($\tau_{\bar{p}} > 0.28$ yr). ²⁷ The best current laboratory limit is that of the APEX Collaboration at the Fermilab \bar{p} storage ring ($\tau_{\bar{p}} > 50$ kyr for $\bar{p} \rightarrow \mu^- X$ and 300 kyr for $e^- \gamma$). ²⁹ A proposed APEX II experiment would be able to reach \bar{p} lifetime limits of

1–10 Myr, comparable to the cosmic ray limit.^b

Since the CPT symmetry holds in LRQFT under the assumptions of Poincaré invariance, locality, microcausality, and vacuum uniqueness, modification of basic physics would be necessary to break it.^{30,31} Within QFT, an extensive formalism and phenomenology of Lorentz and CPT violation has been developed by Kostelecký and collaborators.³² String theory at first glance might seem to provide a natural way to violate locality, but perturbative string dynamics has been shown to preserve CPT in the field theory target space after compactification.³³ *Non-perturbative* string effects associated with compactification may evade this result.³⁴ Extended quantum mechanics, with non-unitary time evolution, violates CPT in general, by violating locality and/or Poincaré symmetry. Controversial proposals of non-unitary evolution have been put forward as natural consequences of quantum gravity and information loss in the presence of spacetime horizons.³⁵ Non-unitary effects have been powerfully limited in the very well-measured $K^0-\bar{K}^0$ system³⁶ (to a few parts in 10^{16}), but not well at all in other systems, particularly baryons.³⁷

The most plausible source of CPT violation lies beyond the Planck scale, based on strings or some other quantum theory of gravity, because of the necessary generalization beyond global Poincaré symmetry. Typically such effects are thought of as suppressed by the large Planck mass $M_{\text{Pl}} \sim 10^{19}$ GeV. But if gravity is fundamentally associated with “large” extra dimensions acting at mass scales as low as 1 TeV,³⁸ the CPT-violating mechanisms may not be that suppressed at accessible energies.

2 Measurements of Cosmic Ray Antiprotons

Detection of CR antiprotons has gone through three distinct phases, following the proposal of Gaisser and Levy to search for \bar{p} secondaries.³ All but recent space-based experiments have been mounted on high-altitude balloons. The measurements are conventionally quoted as the \bar{p}/p ratio of fluxes, convenient because a number of theoretical and experimental uncertainties cancel: the overall IS primary p flux normalization uncertainty, the overall detector flux normalization uncertainty, and (at $K \gtrsim 500$ MeV) diffusive modulation of both fluxes (see below).

The first two Western experiments (those of Golden *et al.* and Buffington *et al.*) detected \bar{p} signals at a level higher than the standard secondary prediction.^{39,40} These early experiments detected \bar{p} 's by energy calorimetry (the deceleration and annihilation of the \bar{p} 's in the balloon), but lacked def-

^bAll lifetime limits quoted here are at 90% C.L.

inite identification by a magnetic spectrometer. Of particular concern is the background of kaons in the detector, as $m_K \lesssim m_p$.

Stimulated by the possibility of an excess of CR \bar{p} 's, a number of groups completed measurements in the 1970s and 1980s with better particle identification. The PBAR and LEAP groups established upper limits on the CR \bar{p} flux contradicting the first-generation experiments.^{41,42} Roughly contemporaneous, the Soviet group of Bogomolov *et al.* reported three flux measurements (from the periods 1972-77, 1984-85, and 1986-88) consistent with standard secondary predictions.^{43,44,45}

2.1 Abundance & Spectrum of Antiprotons

The third generation of experiments came in the 1990s and included markedly better particle detection by magnetic spectrometer, of quality comparable to accelerator experiments. From 1991 to 1997, the MASS (1991), IMAX (1992), CAPRICE (1994), and BESS (1993, 1995, 1997) collaborations have made clean measurements of the CR \bar{p} flux with low backgrounds.^{46,47,48,49,50,51}

The analysis presented here is based on all refereed and published measurements not contradicted by later measurements with better detectors (Table 1).²⁸ Figure 7 shows the selected measurements compared with the ILDM prediction for IS fluxes. The disagreement evident in the figure is explicable by heliospheric modulation. Figure 8 compares the modulated ILDM predictions with the measured fluxes. This figure makes the comparison by renormalizing the measured fluxes to a single epoch (July 1995, chosen as roughly the most recent heliomagnetic minimum) and using the prediction for that epoch. Our analysis did not use measurements with $K < 500$ MeV because of the large and difficult-to-calculate diffusion modulation in that energy range.

2.2 Implications^{28,37}

The most basic result implied by Table 1 and Figure 8 is the standard \bar{p} secondary flux alone, from a realistic ILDM, can account for the observed flux in the relevant energy range, within uncertainties. If variant Galactic transport mechanisms (such as reacceleration or shrouded sources⁷) or exotic \bar{p} sources are at work in this K range, their effects are too small to see at this time. (A hint of reacceleration may be visible in the range $K \simeq 2$ –5 GeV by distortion of the spectrum evident in Figure 8, but the effect is not significant within uncertainties.) A second, less obvious, result is a limit on the intrinsic decay lifetime of the antiproton: $\tau_{\bar{p}} > 0.8$ Myr, the best limit currently feasible. While the exclusion of the $K < 500$ MeV spectrum does *not* significantly affect the $\tau_{\bar{p}}$ limit, it does limit conclusions about the absence

Table 1. Summary of cosmic ray \bar{p} measurements not contradicted by later experiments. Adapted from Geer and Kennedy.²⁸

Experiment	Field Pol. ^a	Flight Date	KE Range (GeV)	Candidates	Back-ground	Observed \bar{p}/p Ratio	Prediction ^b
Golden et al. 1979 [†]	+	June 1979	5.6 – 12.5	46	18.3	$(5.2 \pm 1.5) \times 10^{-4}$	–
Bogomolov et al. 1979 [†]	+	1972-1977	2.0 – 5.0	2	–	$(6 \pm 4) \times 10^{-4}$	–
Bogomolov et al. 1987 [‡]	–	1984-1985	0.2 – 2.0	1	–	$(6_{-5}^{+14}) \times 10^{-5}$	–
Bogomolov et al. 1990 [‡]	–	1986-1988	2.0 – 5.0	3	–	$(2.4_{-1.3}^{+2.4}) \times 10^{-4}$	–
MASS91 ⁴⁶	+	Sep. 1991	3.70–19.08	11	3.3	$(1.24_{-0.51}^{+0.68}) \times 10^{-4}$	1.3×10^{-4}
IMAX ^{‡ 47}	+	July 1992	0.25 – 1.0	3	0.3	$(3.14_{-1.9}^{+3.4}) \times 10^{-5}$	1.5×10^{-5}
IMAX ⁴⁷	+	July 1992	1.0 – 2.6	8	1.9	$(5.36_{-2.4}^{+3.5}) \times 10^{-5}$	6.5×10^{-5}
IMAX ⁴⁷	+	July 1992	2.6 – 3.2	5	1.2	$(1.94_{-1.1}^{+1.8}) \times 10^{-4}$	1.1×10^{-4}
BESS93 ^{‡ 48}	+	July 1993	0.20 – 0.60	7	~ 1.4	$(5.2_{-2.8}^{+4.4}) \times 10^{-6}$	8.9×10^{-6}
CAPRICE ⁴⁹	+	Aug. 1994	0.6 – 2.0	4	1.5	$(2.5_{-1.9}^{+3.2}) \times 10^{-5}$	3.5×10^{-5}
CAPRICE ⁴⁹	+	Aug. 1994	2.0 – 3.2	5	1.3	$(1.9_{-1.0}^{+1.6}) \times 10^{-4}$	1.1×10^{-4}
BESS95 ^{‡* 50}	+	July 1995	0.175 – 0.3	3	0.17	$(7.8_{-4.8}^{+8.3}) \times 10^{-6}$	–
BESS95 ^{‡* 50}	+	July 1995	0.3 – 0.5	7	0.78	$(7.4_{-3.3}^{+4.7}) \times 10^{-6}$	1.1×10^{-5}
BESS95 ^{* 50}	+	July 1995	0.5 – 0.7	7	1.4	$(7.7_{-3.7}^{+5.3}) \times 10^{-6}$	5.5×10^{-6}
BESS95 ^{* 50}	+	July 1995	0.7 – 1.0	11	2.8	$(1.01_{-4.3}^{+5.7}) \times 10^{-5}$	1.3×10^{-5}
BESS95 ^{* 50}	+	July 1995	1.0 – 1.4	15	3.5	$(1.99_{-0.73}^{+0.91}) \times 10^{-5}$	3.1×10^{-5}

^a Northern hemisphere heliomagnetic polarity: + = outward field.

^b ILDM prediction with $V_W(\text{eq/polar}) = 400/750 \text{ km sec}^{-1}$, $B_\odot = 4.5 \text{ nT}$.

[†] Not shown in Figure 7 or used in analysis. [‡] Not used in analysis. * Statistical and systematic uncertainties on ratio added in quadrature.

of exotic \bar{p} sources, as these would have their largest effect relative to the standard secondaries precisely at such low K .

A short \bar{p} lifetime $\tau_{\bar{p}} \lesssim 10 \text{ Myr}$ (Galactic CR storage time) would of course indicate CPT violation. The two pictures of CPT violation introduced in subsection 1.3 are: modification of LRQFT within ordinary quantum mechanics, and non-standard quantum mechanics (NSQM) with non-unitary time evolution. If only one new mass scale is relevant to the CPT violation, lower limits can be placed on such scales. In Table 2, the limiting CPT-violating scales associated with modified QFT (M_X) and NSQM (M_Y) are shown, assuming $\tau_{\bar{p}} = 10 \text{ Myr}$. The \bar{p} lifetime is assumed related to each scale by simple mass dimensions. For modified QFT, $\Gamma_{\bar{p}} = m_p(m_p/M_X)^n$; while for NSQM, $\Gamma_{\bar{p}} =$

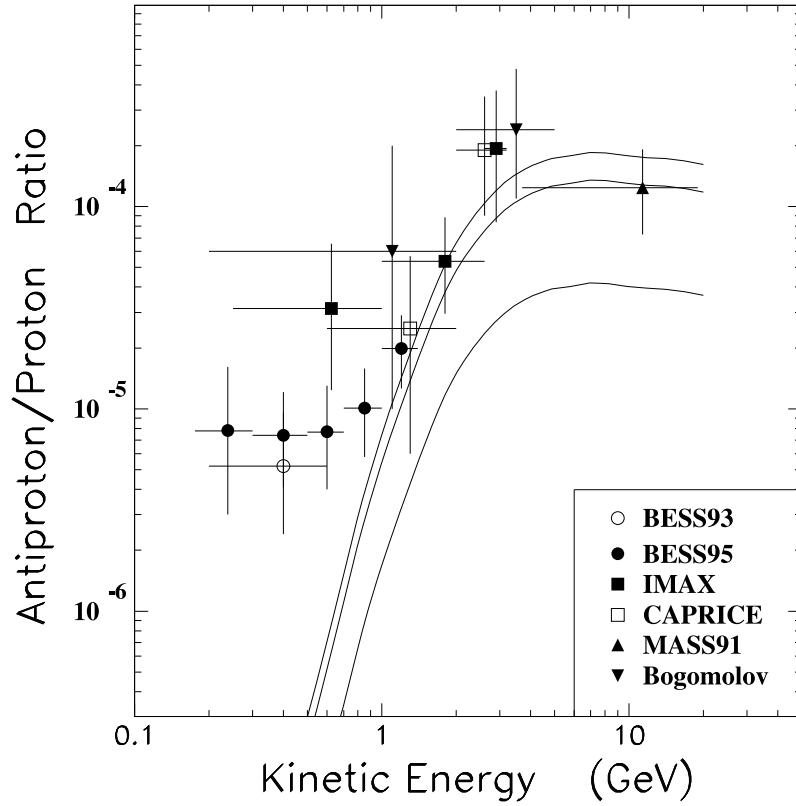


Figure 7. Measured \bar{p}/p spectral flux ratios, compared with *unmodulated* IS CR \bar{p} flux predicted by ILDM (see text).²⁸

$(m_p/2)(m_p/M_Y)^k$. It is interesting to note that the *largest* M_X lower bound is $\mathcal{O}(M_{\text{Pl}})$, while the scales of order the “intermediate” scale (10^8 – 10^{12} GeV) are possible, as well as scales \sim TeV. The last scale may not be unreasonably low in the context of “large” extra dimensional gravity.³⁸

3 Future Developments and Prospects

Uncertainties intrinsic to cosmic ray analysis will probably limit deduction of antimatter properties to about the level already achieved. But the search for exotic sources of primary \bar{p} 's is still open, especially at low energy.

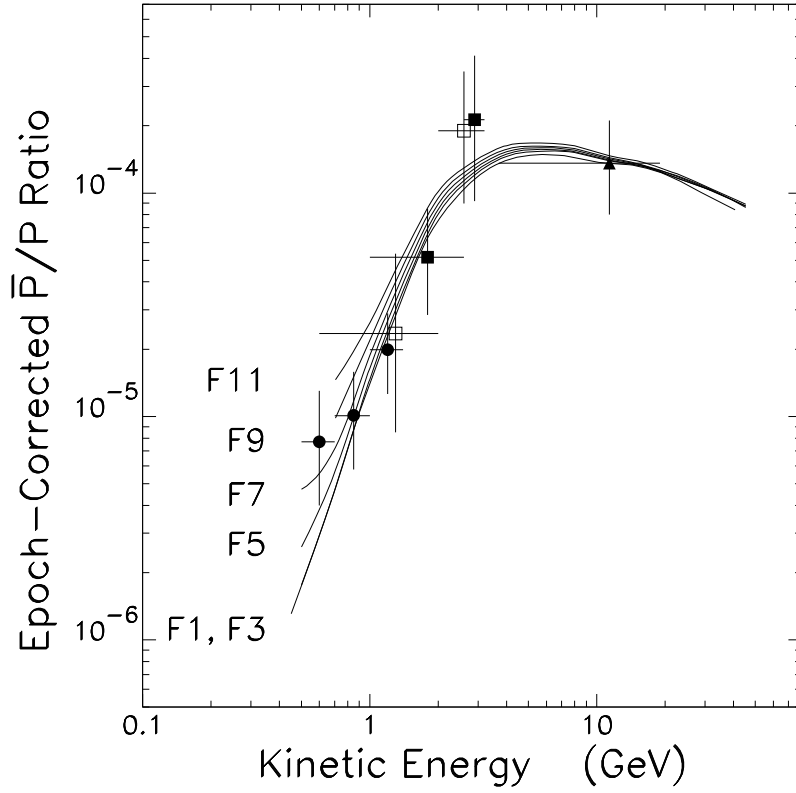


Figure 8. Measured \bar{p}/p spectral flux ratios corrected with heliospheric modulation to common epoch (July 1995), compared with modulated prediction of IS CR \bar{p} flux in ILDM (see text).²⁸

Table 2. CPT - and B -violating scale limits associated with p lifetime $\tau_p = 10^{32}$ yr and \bar{p} lifetime $\tau_{\bar{p}} = 10^7$ yr (see text).³⁷

n	M_X (GeV)	k	M_Y (GeV)
5	2×10^{19}	1	2×10^{63}
6	4×10^9	2	5×10^{31}
7	3×10^6	3	1×10^{21}
8	6×10^4	4	7×10^{15}
9	7×10^3	5	5×10^{12}
10	2×10^3	6	4×10^{10}

3.1 More and Better Measurements

Future measurement of the medium energy range ($K = 0.5\text{--}10$ GeV) will define that part of the spectrum better, but it the spectral shape at the two extremes that is critical for exotic \bar{p} searches.

A number of experiments have already taken recent data not yet published. These include the CAPRICE (1998) and HEAT (1999) balloons, as well as the prototype AMS (1998) and PAMELA (1995 and 1997) systems tested on Space Shuttle STS-91 and the Mir space station, respectively.^{52,53} These experiments can and have searched for positrons and $A > 1$ antinuclei as well. The HEAT- \bar{p} 99 data are especially of interest because of their large energy range ($K = 4\text{--}50$ GeV).

The PAMELA instrument, after being tested in prototype on the Mir space station, is scheduled to fly on an unmanned satellite (the Russian-Italian Resurs-Arktika 4) for three years, starting in 2002.⁵³ It can detect e^+ , \bar{p} , and $\overline{\text{He}}$ at a relative sensitivity of better than one part in 10^7 over a range $K = 0.1\text{--}150$ GeV. The full AMS instrument is scheduled for the International Space Station Alpha starting in 2005, also for three years, with an antiparticle/antinucleus sensitivity of one part in 10^6 for $E > 5$ GeV.

The MASS91 collaboration have also reanalyzed their data and released a new version divided into three energy bins, instead of one.⁵⁴ These three experiments (MASS91, HEAT, and PAMELA) will decisively address the paucity of data at the highest energies and define the spectrum in that range.

3.2 Production & Propagation: Importance of the Low-Energy Spectrum

The low-energy range is already being mapped out by the BESS experiment, in particular in the 1995 and 1997 data sets. Repeated, reliable measurement of the low-energy spectrum is the most important task in the contemporary period of \bar{p} measurements, followed closely by reliable measurement of the high-energy fall-off. The presence of exotic primary \bar{p} 's in this range should be detectable with the current or next generation of experiments.

The main obstacles to conclusive limits on a non-standard \bar{p} flux at low energy are now theoretical. There are two crucial effects needing clarification for such a signal to be found or ruled out. The first is the “subthreshold” \bar{p} production on IS He-4 target nuclei. The status of previous estimates of this effect^{5,6} has been changed in the last decade by laboratory measurements of the \bar{p} production on heavy target nuclei,⁵⁵ providing evidence for a scaling relation between the $A > 1$ and $A = 1$ cases. Recent calculations²³ have begun to take account of these data, and further work is under way to develop a simple nuclear model.⁵⁶

The second is providing a complete heliospheric modulation calculation that includes diffusion, as well as the wind and magnetic drift. The present gap in the literature is defined on one side by thorough modulation calculations applied to low-energy CRs ($K < 100$ MeV) ¹³ and on the other by accurate modulation done at higher energies ($K > 500$ MeV) without diffusion. ²⁸ Approximate calculations without magnetic drift are available, ¹² but the charge-dependent magnetic drift is essential to predicting the \bar{p}/p ratio correctly. A full calculation covering $K \lesssim 100$ MeV to 500 MeV is essential to proper interpretation of the BESS data. ⁵⁷

Cosmic ray antimatter measurements are undergoing exciting developments that will define much of our future understanding of the composition of our Galaxy and of basic symmetries of Nature. Perhaps within 10 years, precise cosmic ray measurements will be a mature subject, along with the ripening of other types of particle astrophysics.

Acknowledgments

The author thanks the PASCOS 99 meeting organizers at UC Davis for the opportunity to present these results, based on work done in collaboration with Stephen Geer (Fermilab). This work was supported by the U.S. DOE under grants DE-FG02-97ER41029 (Univ. Florida) and DE-AC02-76CH03000 (Fermilab), NASA under grant NAG5-2788 (Fermilab), and the Institute for Fundamental Theory at the Univ. Florida, and was greatly enhanced by conversations with J. R. Jokipii (Lunar & Planetary Laboratory, Univ. Arizona), E. J. Smith (Jet Propulsion Laboratory), V. A. Kostelecký (Indiana Univ.), and M. Kamionkowski (CalTech). The author is also grateful to the NASA/Fermilab Theoretical Astrophysics group and the Telluride Summer Research Center for their hospitality.

References

1. P. C. Frisch, *Amer. Sci.* **88**(1), 52 (2000); ACE spacecraft: <http://www.srl.caltech.edu/ACE/> .
2. PAMELA experiment: http://msia02.msi.se/group_docs/astro/research/PAMELA.html .
3. T. K. Gaisser and E. H. Levy, *Phys. Rev. D* **10**, 1731 (1974).
4. S. A. Stephens, *Astrophys. Space Sci.* **76**, 87 (1981); S. A. Stephens and R. L. Golden, *Space Sci. Rev.* **46**, 31 (1987).
5. W. R. Webber and W. S. Potgieter, *Astrophys. J.* **344**, 779 (1989).
6. T. K. Gaisser and R. K. Schaefer, *Astrophys. J.* **394**, 174 (1992).

7. T. K. Gaisser, *Cosmic Rays and Particle Physics* (Cambridge University Press, Cambridge, 1990) chapter 10; J. F. Ormes *et al*, in *Proc. 1994 Snowmass Summer Study: Particle and Nuclear Astrophysics and Cosmology in the Next Millenium*, ed. E. W. Kolb and R. D. Peccei (World Scientific, Singapore, 1995) 312.
8. W. R. Webber, M. A. Lee, and M. Gupta, *Astrophys. J.* **390**, 96 (1992).
9. M. .S. Longair, *High Energy Astrophysics*, 2nd ed. (Cambridge University Press, Cambridge, 1992), 2 vols.
10. P. Chardonnet *et al*, *Phys. Lett. B* **384**, 161 (1996); A. Bottino *et al*, *Phys. Rev. D* **58**, 123503 (1998).
11. E. N. Parker, *Interplanetary Dynamical Processes* (Interscience Publishers, New York, 1963).
12. L. A. Fisk and W. I. Axford, *J. Geophys. Res.* **74**, 4973 (1969); L. A. Fisk, *Geophys. Res.* **76**, 221 (1971).
13. J. R. Jokipii and B. Thomas, *Astrophys. J.* **243**, 1115 (1981); J. Kóta and J. R. Jokipii, *Science* **268**, 1024 (1995); L. A. Fisk *et al.*, *Space Sci. Rev.* **83**, 1ff (1998).
14. IMP-8 spacecraft: <http://nssdc.gsfc.nasa.gov/space/imp-8.html> .
15. Ulysses spacecraft: <http://ulysses.jpl.nasa.gov/> .
16. H. Bloemen, *Ann. Rev. Astron. Astrophys.* **27469**, 1989 (.)
17. G. Steigman, *Ann. Rev. Astron. Astrophys.* **14**, 399 (1976); W. H. Kinney, E. W. Kolb, and M. S. Turner, *Phys. Rev. Lett.* **79**, 2620 (1997).
18. E. W. Kolb and M. S. Turner, *The Early Universe* (Addison-Wesley, Redwood City, CA, 1990) chapter 9; D. Spergel, in *Unsolved Problems in Astrophysics*, ed. J. N. Bahcall and J. P. Ostriker (Princeton University Press, Princeton, 1997) chapter 11.
19. J. Ellis, J. S. Hagelin, D. V. Nanopoulos, K. Olive, and M. Srednicki, *Nucl. Phys. B* **238**, 453 (1984).
20. J. Silk and M. Srednicki, *Phys. Rev. Lett.* **50**, 624 (1984).
21. G. Jungman and M. Kamionkowski, *Phys. Rev. D* **51**, 3121 (1995); G. Jungman, M. Kamionkowski, and K. Griest, *Phys. Rep.* **267**, 195 (1996).
22. S. W. Hawking, *Commun. Math. Phys.* **43**, 199 (1975).
23. L. Bergström, J. Edsjö, and P. Ullio, LANL astro-ph/9902012; and in *Proc. 26th Intl. Cosmic Ray Conf. (ICRC), Salt Lake City*, ed. D. Kieda, M. Salamon, and B. Dingus (American Institute of Physics, College Park, MD, 2000), vol. 2, 285.
24. P. Kiraly *et al*, *Nature* **293**, 120 (1981).
25. E. Perez, Y. Sirois, and H. Dreiner, in *Proc. Workshop Future Physics at HERA*, ed. G. Ingelman, A. De Roeck, and R. Klanner (DESY, Hamburg,

- 1997), vol. 1, 295, LANL hep-ph/9703444.
26. EGRET telescope: <http://coss.gsfc.nasa.gov/code661/code661.html> .
 27. C. Caso *et al* (Particle Data Group), *Euro. Phys. J.* **C3**, 613 (1998) and <http://pdg.lbl.gov/> .
 28. S. H. Geer and D. C. Kennedy, LANL astro-ph/9809101; and *Astrophys. J.* **532**, 648 (2000).
 29. S. Geer *et al* (APEX Collaboration), *Phys. Rev. Lett.* **72**, 1596 (1994); M. Hu *et al* (APEX Collaboration), *Phys. Rev. D* **58**, 111101 (1998); S. Geer *et al* (APEX Collaboration), *Phys. Rev. Lett.* **84**, 590 (2000).
 30. R. F. Streater and A. S. Wightman, *PCT, Spin and Statistics, and All That* (W. A. Benjamin, New York, 1964).
 31. *Proc. CPT and Lorentz Symmetry Meeting*, ed. V. A. Kostelecký (World Scientific, Singapore, 1999).
 32. D. Colladay and V. A. Kostelecký, *Phys. Rev. D* **55**, 6760 (1997) and *Phys. Rev. D* **58**, 116002 (1998).
 33. V. A. Kostelecký and R. Potting, *Nucl. Phys. B* **359**, 545 (1991).
 34. J. Polchinski, *String Theory* (Cambridge University Press, Cambridge, 1998) chapter 18.
 35. S. W. Hawking, *Phys. Rev. D* **14**, 2460 (1976); D. N. Page, *Gen. Rel. Grav.* **14**, 299 (1982); T. Banks, L. Susskind, and M. E. Peskin, *Nucl. Phys. B* **244**, 125 (1984); J. Ellis *et al*, *Nucl. Phys. B* **241**, 381 (1984); P. Huet and M. E. Peskin, *Nucl. Phys. B* **434**, 3 (1995).
 36. R. Adler *et al* (CPLEAR Collaboration) and J. Ellis *et al*, *Phys. Lett. B* **364**, 239 (1995).
 37. D. C. Kennedy, *Mod. Phys. Lett.* **A14**, 849 (1999).
 38. J. D. Lykken, *Phys. Rev. D* **54**, 369 (1996); N. Arkani-Hamed, S. Dimopoulos, and G. Dvali, *Phys. Rev. D* **59**, 086004 (1999); L. Randall and R. Sundrum, *Phys. Rev. Lett.* **83**, 4690 (1999).
 39. R. L. Golden *et al*, *Phys. Rev. Lett.* **43**, 1196 (1979).
 40. A. Buffington *et al*, *Astrophys. J.* **248**, 1179 (1981).
 41. S. P. Ahlen *et al* (PBAR Collaboration), *Phys. Rev. Lett.* **61**, 145 (1988); M. H. Salamon *et al* (PBAR Collaboration), *Astrophys. J.* **349**, 78 (1990).
 42. R. E. Streitmatter *et al* (LEAP Collaboration), in *Proc. 21st Intl. Cosmic Ray Conf. (ICRC), Adelaide* (Univ. Adelaide, Adelaide, 1990), vol. 3, 277.
 43. E. A. Bogomolov *et al*, in *Proc. 16th Intl. Cosmic Ray Conf. (ICRC), Kyoto* (Inst. Cosmic Ray Research, Tokyo, 1979), vol. 1, 330.
 44. E. A. Bogomolov *et al*, in *Proc. 20th Intl. Cosmic Ray Conf. (ICRC), Moscow* (Nauka, Moscow, 1987), vol. 2, 72.

45. E. A. Bogomolov *et al*, in *Proc. 21st ICRC*, vol. 3, 288.
46. M. Hof *et al* (MASS Collaboration), *Astrophys. J.* **467**, L33 (1996).
47. J. W. Mitchell *et al* (IMAX Collaboration), *Phys. Rev. Lett.* **87**, 3057 (1996).
48. K. Yoshimura *et al* (BESS Collaboration), *Phys. Rev. Lett.* **75**, 3792 (1995); A. Moiseev *et al* (BESS Collaboration), *Astrophys. J.* **474**, 479 (1997).
49. M. Boezio *et al* (CAPRICE Collaboration), *Astrophys. J.* **487**, 415 (1997).
50. H. Matsunaga *et al* (BESS Collaboration), *Phys. Rev. Lett.* **81**, 4052 (1998).
51. S. Orito *et al* (BESS Collaboration), *Phys. Rev. Lett.* **84**, 1078 (2000).
52. Flown experiments soon to be published: C. R. Bower *et al* (HEAT Collaboration), M. L. Ambriola *et al* (CAPRICE Collaboration), and J. Alcaraz *et al* (AMS Collaboration), in *Proc. 26th ICRC*, vol. 5, resp. 13, 17, and 88.
53. Experiments soon to fly: S. Ahlen *et al* (AMS Collaboration), *Nucl. Instrum. Meth.* **A350**, 35 (1994); O. Adriani *et al* (PAMELA Collaboration), in *Proc. 26th ICRC*, vol. 5, 96.
54. G. Basini *et al* (MASS Collaboration), in *Proc. 26th ICRC*, vol. 3, 77.
55. A. Sibirtsev *et al*, *Nucl. Phys. A* **632**, 131 (1998)
56. D. C. Kennedy and G. Miller, work in progress.
57. S. H. Geer and D. C. Kennedy, work in progress.